

Control of a Two-Link Robot to Achieve Sliding and Hopping Gaits

Matthew D. Berkemeier*

Ronald S. Fearing†

Electronics Research Laboratory
Department of Electrical Engineering and Computer Sciences
University of California, Berkeley, CA 94720

Abstract

In this paper a new example of a hopping robot is considered, consisting simply of two links (the end of one link acts as the foot) joined by an actuated, revolute joint. For the stance phase a nonlinear controller is derived that maintains the balance of the robot and periodically accelerates the center of mass vertically. For large enough oscillations the robot can slide or take off. If flight is achieved, the drift caused by non-zero angular momentum can typically be canceled by rotating the actuated joint an integral number of times, and the robot can land in the same configuration in which it took off. This is due to the holonomy of a single rotation of the actuated joint. Results of simulations are presented in which the robot achieves both sliding and hopping gaits.

1 Introduction

Most of the previous work on hopping in robotics has focused on the mechanism designed and built by Raibert [12]. His design consisted of a body joined to an actuated, prismatically-jointed leg by an actuated, revolute joint (Figure 1). It was capable of hopping in place, hopping at various forward speeds, and leaping over small obstacles. Two-legged and four-legged versions were also built.

Bühler and Koditschek, Vakakis and Burdick, M'Closkey and Burdick, and Li and He [2, 13, 10, 7] all studied the hopping cycle of Raibert's robot. By considering simplified dynamics of the hopper, various predictions could be made about the hopper's behavior as a function of parameters. Among the interesting results were the existence of stable limit cycles with doubly periodic Poincaré maps (so-called "limping gaits"). More importantly, the approaches used should be applicable to general legged robots. Li and Montgomery [8] studied the dynamics of the flight

*Supported by NSF grants IRI-9014490 and IRI-9157051.

†Supported by NSF grant IRI-9157051.

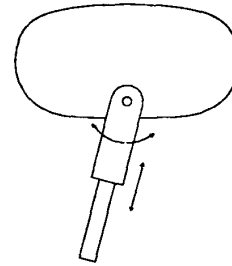


Figure 1: Schematic of Raibert's Hopper

phase for Raibert's robot and considered the problem of optimally performing a somersault in the air by using the holonomy generated by internal motions. Although the goal in this paper is also to use internal motions to achieve a particular orientation while in flight, no attempt is made to perform the motions in an optimal fashion.

Recently, Kanai and Yamafuji [6] have built a three-link hopping mechanism where, apparently, one revolute joint was used to balance and the other was used to provide thrust for jumps.

Much was learned from studying Raibert's mechanism. However, it is important to consider new examples. Typically, it is only by comparing the results of many specific examples of a phenomenon that a general understanding of the unifying principles can be realized. In this paper a new example of a hopping robot is considered, consisting simply of two links (the end of one link acts as the foot) joined by an actuated, revolute joint. Unlike with Raibert's hopper, it is not immediately clear how to achieve a hopping gait.

It is necessary to divide the control problem into two parts: control of the robot in the stance phase and in the flight phase. While in the stance phase, as long as the foot does not slide, the dynamics of the two-link hopper are identical to those of a double pendulum with actuated second joint (Figure 3). An example of this mechanism, named the "Acrobot," was built in

1988 in the UC Berkeley EECS Robotics Lab. Indeed, the Acrobot provided part of the inspiration for this research. Hauser and Murray have already considered the problem of controlling this mechanism in [4]. They applied the nonlinear control method of approximate linearization to cause the Acrobot to move along the set of inverted equilibrium positions, i.e., those positions where the center of mass was directly above the free joint. The method worked well in simulations but required slow motions, which ruled it out as a possibility for hopping. In this paper a nonlinear controller is derived that maintains the balance of the Acrobot in inverted positions and periodically accelerates the center of mass vertically (for suitably chosen masses and link lengths). For large enough oscillations this control can cause the hopping robot to slide or take off.

If flight is achieved, the drift caused by non-zero angular momentum can typically be canceled by rotating the actuated joint an integral number of times, and the robot can land in the same configuration in which it took off. This is due to the holonomy of a single rotation of the actuated joint.

The paper is organized as follows: Section 2 gives the details of the control schemes used for stance and flight phases. In Section 3 simulations of the two-link robot are presented in which the robot achieves both sliding and hopping gaits. The work is summarized and future research is described in Section 4.

2 Control Strategies for the Two-Link Robot

In this section the control schemes for stance and flight phases are described. Throughout this section the approach of Nijmeijer and van der Schaft [11, Chapter 12], which deals specifically with *mechanical* control systems is used. The basic requirement for using this approach is that the dynamical equations come from Hamilton's equations.

The control systems for both Subsections 2.1 and 2.2 take the form

$$\dot{x} = X_{H_0}(x) - X_{H_1}(x)u$$

with $x \in M$, the $2n$ -dimensional phase space manifold. X_{H_i} , $i = 0, 1$, is the vectorfield associated with the Hamiltonian function H_i . u is the torque at the actuated joint.

The *standard Poisson bracket* in local coordinates, $(q, p) = (q_1, \dots, q_n, p_1, \dots, p_n)$, is given by

$$\{F, G\}(q, p) = \sum_{i=1}^n \left(\frac{\partial F}{\partial p_i} \frac{\partial G}{\partial q_i} - \frac{\partial F}{\partial q_i} \frac{\partial G}{\partial p_i} \right) (q, p)$$

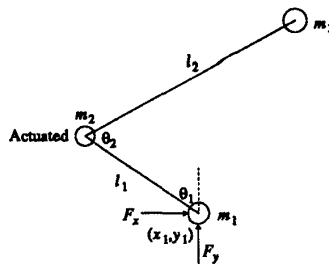


Figure 2: Coordinates for Two-Link Robot

The q_i 's are the generalized configuration coordinates, and the p_i 's are the associated generalized momenta. Notice that $\{F, G\}(q, p)$ is the derivative of the function G in the direction $X_F(q, p)$. The standard Poisson bracket is assumed throughout the remainder of this section.

Figure 2 gives the coordinates used for the two-link robot.

2.1 Stance Phase

Control of the Acrobot (which has the same dynamics as the two-link robot if forces are kept within the friction cone) is difficult since the system must maintain its balance while at the same time accelerate its center of mass upward to slide or take off. With only one input it is not immediately obvious how this can be accomplished. In this subsection a nonlinear controller is described which is capable of accomplishing these goals for *appropriately chosen masses and link lengths*. It is assumed that the controller has access to all four states. In actual implementation the leg's angle and angular velocity could be measured by attaching a passive "ski" with encoder to the foot. A gyroscope could also be used and would have the advantage of supplying the leg's angle and angular velocity even while the foot was not on the ground.

Let ϕ be some constant. If one solves the equations

$$\begin{aligned} (1) \quad 2\theta_1 + \theta_2 &= \phi \\ (2) \quad 2\dot{\theta}_1 + \dot{\theta}_2 &= \{H_0, 2\theta_1 + \theta_2\} = 0 \end{aligned}$$

for θ_2 and p_{θ_2} in terms of θ_1 and p_{θ_1} and then substitutes them into the equations of motion for the Acrobot, the equations for $\dot{\theta}_1$ and \dot{p}_{θ_1} become

$$\begin{aligned} (3) \quad \dot{\theta}_1 &= \frac{p_{\theta_1}}{(m_2 + m_3)l_1^2 - m_3l_2^2} \\ (4) \quad \dot{p}_{\theta_1} &= (m_2 + m_3)gl_1 \sin \theta_1 + m_3gl_2 \sin(\theta_1 - \phi) \end{aligned}$$

These equations are basically those of a single degree-of-freedom pendulum since the two $\sin(\cdot)$ terms can be

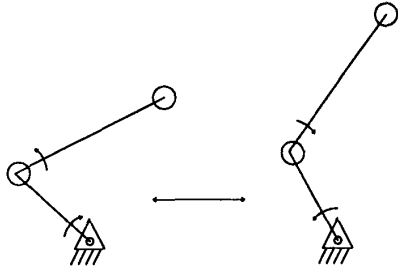


Figure 3: Hopping Motion

combined into a single $\sin(\cdot)$ term using trigonometric identities. Notice that a particular orbit of Equations 1 - 4 can be specified by two parameters. One is the constant ϕ , and this specifies the equilibrium point about which the oscillation in Equations 3 and 4 occurs. The other parameter corresponds to the magnitude of the oscillation. Depending on the choices of the masses, link lengths, and the two just-mentioned parameters, a variety of motions are observed. In particular, motions suitable for hopping can be achieved. Figure 3 attempts to convey one of these motions (Also see the simulations in Section 3).

First, a feedback will be found to maintain $(2\ddot{\theta}_1 + \ddot{\theta}_2)(t) = 0 \forall t$. Clearly, with this feedback and with initial conditions on a desired orbit of Equations 1 - 4, the states will continue to follow this orbit. In the field of nonlinear control this is the problem of finding the input to produce the *zero dynamics* of the output function $2\theta_1 + \theta_2 - \phi$. Next, an additional feedback term to include is described so that even with initial states not exactly on a desired orbit, the motion will asymptotically approach the orbit.

Since

$$2\ddot{\theta}_1 + \ddot{\theta}_2 = \{H_0, \{H_0, 2\theta_1 + \theta_2\}\} - \{H_1, \{H_0, 2\theta_1 + \theta_2\}\}u$$

the desired feedback is given by

$$u = \frac{\{H_0, \{H_0, 2\theta_1 + \theta_2\}\}}{\{H_1, \{H_0, 2\theta_1 + \theta_2\}\}}(x) + v = \alpha(x) + v$$

where v is the input for the transformed system.

Regulation Theory of Isidori [5] is the approach used to converge to a particular orbit of Equations 1 - 4 if the initial conditions are not on the orbit.¹ The application of this theory is particularly simple in this case. Let the Jacobian linearization of the Acrobot equations with the feedback $\alpha(x)$ about a particular equilibrium point be

$$\dot{x} = Ax + bv, \quad A \in \mathbb{R}^{4 \times 4}, \quad b \in \mathbb{R}^4$$

¹Credit for this idea goes to Andy Teel.

Assume that the pair (A, b) is stabilizable, i.e., there exists a row vector k such that all the eigenvalues of $(A + bk)$ have negative real part. Now, let the desired orbit of Equations 1 - 4 be given by $w(\cdot)$. Then the feedback

$$v = k(x - w)$$

causes the system's states to asymptotically converge to a $w(\cdot)$ sufficiently close to the equilibrium point for initial conditions sufficiently close to the equilibrium point. This type of controller is called a *regulator*. The feedback $\alpha(x) + k(x - w)$ was used with a high degree of success in simulations.

2.2 Flight Phase

As in [8] the goal here is to achieve some desired orientation (θ_1) by using internal motions (changes of θ_2 by integral multiples of 2π). However, no attempt is made to satisfy an optimality condition.

If the robot's center of mass is used to give its position while in flight, then the positional dynamics are completely decoupled from the angular dynamics. The positional dynamics are of course trivial; their graph is a parabola. Thus, instead of having to consider the full eight states, only the four states associated with the angular dynamics need to be considered. The ballistic trajectory of the robot does, however, put a time constraint on the problem.

Angular momentum is conserved during the flight phase. This is known as a *nonholonomic constraint* since the equation for angular momentum involves derivatives of the configuration variables, and it cannot be integrated so that it is a function of the configuration variables only. For a classic discussion of an athlete's movements subject to the angular momentum constraint, see Frolich's paper [3]. Much work has been done recently on path planning for systems with nonholonomic constraints; however, the two-link robot is simple enough to yield a straightforward solution.

When Hamilton's equations are used, the conserved quantity is simply p_{θ_1} . From the equations of motion, the following differential relationship can be derived:

$$(5) \quad d\theta_1 = \frac{c_1 p_{\theta_1}}{c_2 + c_3 - 2c_4 \cos \theta_2(t)} dt + \frac{c_4 \cos \theta_2 - c_3}{c_2 + c_3 - 2c_4 \cos \theta_2} d\theta_2$$

$$c_1 = m_1 + m_2 + m_3, \quad c_2 = m_1(m_2 + m_3)l_1^2 \\ c_3 = m_3(m_1 + m_2)l_2^2, \quad c_4 = m_1 m_3 l_1 l_2$$

Integrating this equation gives the relationship between the robot's orientation (θ_1) and its internal angle (θ_2). Consider a change of θ_2 by 2π . Then, the

integral of the second term is called the *geometric phase* or *holonomy*. Clearly, it is the same for any function $\theta_2(\cdot)$ that is used to achieve a change of 2π . The integral of the first term of Equation 5 is called the *dynamic phase*, and its value *does* depend on the choice of $\theta_2(\cdot)$. For the case of $p_{\theta_1} = 0$, there is no dynamic phase. For a mathematically oriented account of phases see the paper by Marsden et al. [9].

Assume it is desired to have the angular coordinates when impact occurs be the same as at takeoff. The simplest solution would be to take off with zero angular momentum. Unfortunately, though, with the controller for the stance phase described in Subsection 2.1, this is virtually impossible. Thus, it is necessary to cancel the drift of the orientation caused by non-zero angular momentum. Since it is desired to land in the same configuration as at takeoff, the time of flight is simply $2v_y/g$, where v_y is the vertical component of the center-of-mass velocity at takeoff. This assumes, of course, that the leg does not prematurely impact the ground. Bounds can be placed on the integral of the first term in Equation 5 by simply replacing $\cos \theta_2$ by ± 1 and then multiplying the term by the time of flight $2v_y/g$. Let these bounds be p_{\min} and p_{\max} , and then define the open set $U \doteq (p_{\min}, p_{\max}) \subset \mathbb{R}$. Let $P : \mathbb{R} \rightarrow S^1$, $p \mapsto p \pmod{2\pi}$, and let ψ_g be the geometric phase. Then, canceling the drift is possible if

$$(6) \quad P(n\psi_g) \in P(U)$$

for some $n \in \mathbb{Z}$. The value of $(-n)$ is the number of times the leg must be rotated.

If a value of n is found to satisfy Equation 6 then a function for $\theta_2(\cdot)$ to exactly cancel the drift can be found, for example, by using a particular set of basis functions and numerically solving for the coefficients.

It is apparent that the controller must cause the actuated joint angle, θ_2 , to track some desired $\theta_{2d}(\cdot)$. This can be accomplished by applying a feedback which linearizes the dynamics of θ_2 . This type of controller is commonly known as a *computed torque* controller.

Since

$$\ddot{\theta}_2 = \{H_0, \{H_0, \theta_2\}\} - \{H_1, \{H_0, \theta_2\}\}u$$

the input

$$u = -\frac{1}{\{H_1, \{H_0, \theta_2\}\}} \left(-\{H_0, \{H_0, \theta_2\}\} + \ddot{\theta}_{2d} - \alpha_1[\{H_0, \theta_2\} - \dot{\theta}_{2d}] - \alpha_2[\theta_2 - \theta_{2d}] \right)$$

produces the error dynamics

$$\ddot{e} + \alpha_1\dot{e} + \alpha_2e = 0, \quad e \doteq \theta_2 - \theta_{2d}$$

Thus, for a choice of α_1 and α_2 which gives poles of the transfer function for the above equation in the left-half plane, the actuated joint angle will asymptotically track $\theta_{2d}(\cdot)$.

3 Simulation Results

In this section results for simulations of both a sliding gait and a hopping gait are presented. A fourth-order Runge-Kutta integration routine with adaptive step size was used to perform the simulations. Values used for the parameters were

$$\begin{aligned} m_1 &= 2 \text{ kg}, \quad m_2 = m_3 = 7 \text{ kg} \\ l_1 &= 0.5 \text{ m}, \quad l_2 = 0.75 \text{ m}, \quad g = 9.8 \text{ m/s}^2 \\ \phi &= (\pi - 0.5) \text{ rad}, \quad \mu_s = 0.5, \quad \mu_d = 0.4 \end{aligned}$$

μ_s and μ_d are the static and dynamic friction coefficients, respectively, for the foot with respect to the ground. Poles for the regulator and computed torque controller were all set to be -5 s^{-1} . Impact was modeled as an instantaneous inelastic collision. Included was the possibility for the foot to instantaneously start sliding upon impact if the impulsive constraint forces were outside the friction cone.

3.1 Sliding Gait

Figure 4 shows the components of the constraint force on the Acrobot while following particular orbits of Equations 1 - 4. The dashed and solid lines are traced in both directions while the orbits are followed. The dot-dashed line in the figure is the static friction cone boundary, $F_y = (1/\mu_s)|F_x|$. Notice that the dashed graph of the constraint force components exits the friction cone on the left side periodically. Thus, it is not surprising that when the controller for the two-link robot tries to follow this motion, the robot starts sliding. It is important that the robot slides only in one direction. For this particular simulation the sliding was in the $+x$ direction. This makes sense since F_x on the two-link robot is not as negative as it needs to be to hold the foot in place.

Figure 5 shows the configuration variables as the robot slides along. The dashed lines are the graphs of the orbit the controller is trying to make the system follow. Notice how well the regulator keeps θ_1 and θ_2 on track even though it is subject to significant disturbances when the robot starts to slide.

In Figure 6 some frames are shown for a movie of the robot in its sliding gait. The sliding takes place close to where the robot reaches its maximum height. The frames are 0.08 s apart.

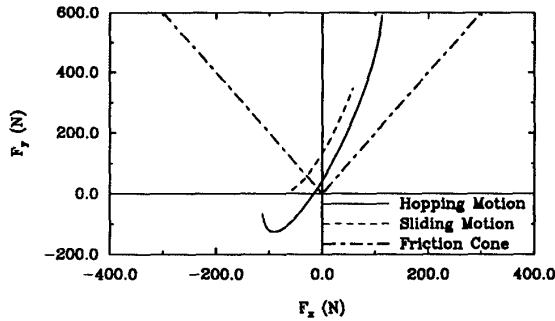


Figure 4: Constraint Forces for Acrobot Oscillations

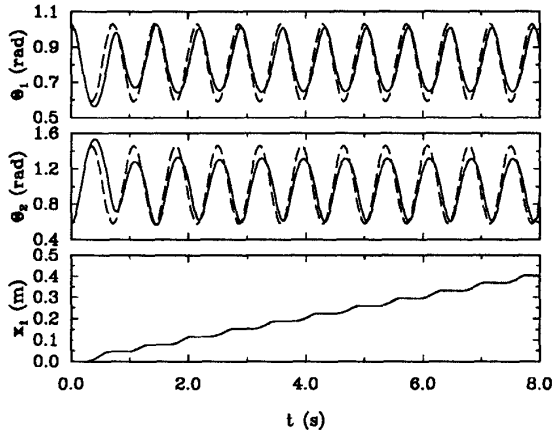


Figure 5: Configuration Variables for Sliding Gait

3.2 Hopping Gait

In Figure 4 the solid curve shows the constraint force components for an oscillation of much larger magnitude than discussed in the previous subsection. The vertical component of the constraint force actually must become negative to hold the foot on the ground. When the controller for the two-link robot attempts to follow the orbit which generated this graph, the foot slides where the curve exits the friction cone, and then the foot lifts off the ground when F_y becomes negative.

Due to the complexity of a hopping gait, only one

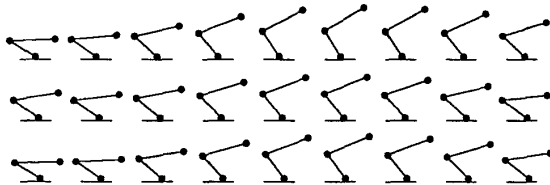


Figure 6: Frames for Sliding Gait

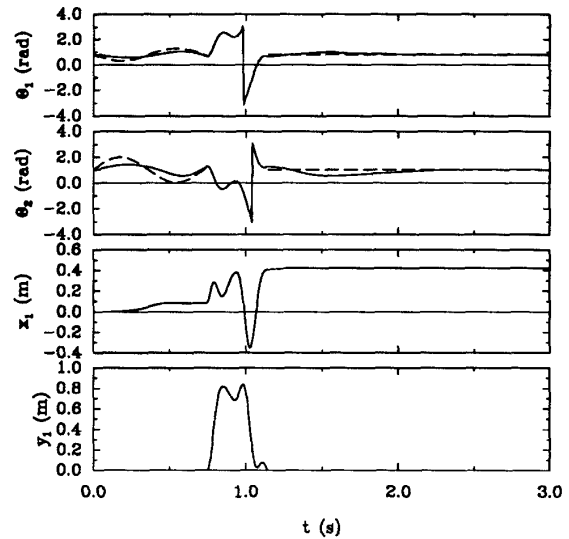


Figure 7: Configuration Variables for Hopping Gait

cycle is shown here. The robot starts at the equilibrium point corresponding to $\phi = \pi - 0.5$ and then is excited by the regulator until it takes off. After rotating its leg once to cancel the drift, the robot lands in the same configuration in which it took off and then returns to the same equilibrium point at which it started. Since the initial and final states are the same (except for x_1), it is clear that this can be repeated as needed for a hopping gait.

Figure 7 shows the configuration variables for the hopping gait. The dashed lines before take-off again show the orbit the regulator is trying to make the robot follow. Notice that some sliding takes place before the robot takes off. Also, notice that at takeoff, the state is actually quite close to the desired state.

The sharp discontinuity in θ_1 and θ_2 while the robot is in flight is due to the fact that the values of these coordinates are shown mod 2π so that it is clear that their values when the robot lands are the same as at takeoff. θ_2 was changed by -2π in a particular manner so that the change in θ_1 was exactly $+2\pi$. Polynomial basis functions were used to find a function $\theta_2(\cdot)$ with this property. Notice in Figure 7 that the foot comes close to touching the ground before the desired orientation is reached. The clearance here probably could be improved by some different function for $\theta_2(\cdot)$. x_1 advances a total of around 0.4 m during this cycle of the hopping gait.

The dashed lines after the landing correspond to the equilibrium point toward which the regulator is steering the robot.

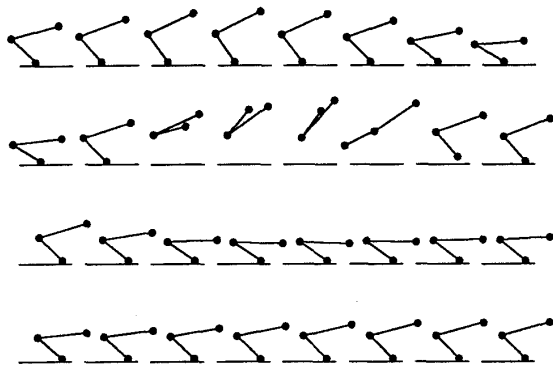


Figure 8: Frames for Hopping Gait

Figure 8 is a series of frames of a movie for the robot performing its hopping gait. Once again, they are 0.08 s apart.

4 Conclusions and Future Work

In this paper a new example of a hopping robot was introduced. Much of the previous research on hopping robots has focused on the mechanism Raibert built; however, it is important that new examples be considered in order to draw general conclusions. Raibert's robot is clearly much easier to control than the two-link robot. Having a springy leg plus an extra degree of freedom accounts for this. Control schemes were described for both the stance and flight phases of the two-link robot. The feedback during stance phase transformed the system into one with dynamics desirable for hopping. For the flight phase rotating the leg an integral number of times could typically enable the robot to land in the same configuration in which it took off. This was due to the holonomy associated with the internal motion of changing θ_2 by 2π . Simulation results showed that the control strategies derived were effective. The robot could slide along the ground and hop.

Future work will include further investigation into the control of the two-link robot. Currently, a two-link mechanism is being constructed to test the simulation results presented here. In addition, similar control strategies used here are being applied to a four-link biped to attempt walking and running. This work will be reported in [1].

Acknowledgements

Much thanks to Richard M. Murray and Andrew R. Teel for discussions of this project and offering valuable suggestions.

References

- [1] M. D. Berkemeier. *Control of Dynamic Gaits in Legged Robots*. PhD thesis, UC Berkeley, Dept. of EECS, 1992.
- [2] M. Bühler and D. E. Koditschek. Analysis of a simplified hopping robot. In *Proc. IEEE Int. Conf. Robotics Automat.*, pp. 817-819, 1988.
- [3] C. Frolich. Do springboard divers violate angular momentum conservation? *Amer. J. Phys.*, 47(7):583-592, July 1979.
- [4] J. Hauser and R. M. Murray. Nonlinear controllers for non-integrable systems: the acrobot example. In *Proc. Amer. Contr. Conf.*, pp. 669-671, 1990.
- [5] A. Isidori. *Nonlinear Control Systems*. Springer-Verlag, New York, 2nd ed. 1989.
- [6] H. Kanai and K. Yamafuji. Posture change and jumping motion of the controlling arm-leg type mobile robot. *Trans. Japan Soc. Mechanical Eng. C*, 57(539):2336-2341, July 1991. (in Japanese).
- [7] Z. Li and J. He. An energy perturbation approach to limit cycle analysis in legged locomotion systems. In *Proc. 29th IEEE Conf. Decision Contr.*, pp. 1989-1994, 1990.
- [8] Z. Li and R. Montgomery. Dynamics and optimal control of a legged robot in flight phase. In *Proc. IEEE Int. Conf. Robotics Automat.*, pp. 1816-1820, 1990.
- [9] J. E. Marsden, R. Montgomery, and T. Ratiu. Reduction, symmetry, and phases in mechanics. *Memoirs Amer. Math. Soc.*, 88(436), Nov. 1990.
- [10] R. T. M'Closkey and J. W. Burdick. An analytic study of simple hopping robots with vertical and forward motion. In *Proc. IEEE Int. Conf. Robotics Automat.*, pp. 1392-1397, 1991.
- [11] H. Nijmeijer and A. J. van der Schaft. *Nonlinear Dynamical Control Systems*. Springer-Verlag, New York, 1990.
- [12] M. H. Raibert. *Legged Robots that Balance*. MIT Press, Cambridge, MA, 1986.
- [13] A. F. Vakakis and J. W. Burdick. Chaotic motions in the dynamics of a hopping robot. In *Proc. IEEE Int. Conf. Robotics Automat.*, pp. 1464-1469, 1990.